frontiers | Frontiers in Earth Science

TYPE Original Research
PUBLISHED 09 January 2023
DOI 10.3389/feart.2022.1107921

OPEN ACCESS

EDITED BY
Kun Ji,
Hohai University, China

REVIEWED BY
Mianshui Rong,
Beijing University of Technology, China
Zhao Xiaofen,
China Earthquake Administration, China

*CORRESPONDENCE
Hongwei Wang,
whw1990413@163.com

SPECIALTY SECTION
This article was submitted to Structural Geology and Tectonics, a section of the journal Frontiers in Earth Science

RECEIVED 25 November 2022
ACCEPTED 08 December 2022
PUBLISHED 09 January 2023

CITATION
Yao X, Zhang P, Zhao Y, Wang H and Wang D (2023), Region-dependent site conditions in China: Evidence from borehole data statistics.
Front. Earth Sci. 10:1107921.
doi: 10.3389/feart.2022.1107921

Region-dependent site conditions in China: Evidence from borehole data statistics

Xinxin Yao[1,2], Peng Zhang[1,2], Yu Zhao[1,2], Hongwei Wang[1,2]* and Daren Wang[1,2]

[1]Key Laboratory of Earthquake Engineering and Engineering Vibration, Institute of Engineering Mechanics, China Earthquake Administration, Harbin, China, [2]Key Laboratory of Earthquake Disaster Mitigation, Ministry of Emergency Management, Harbin, China

Consideration of site effects is vital in modeling and predicting earthquake ground motions. However, site conditions can vary markedly between different localities. The regional dependency of site conditions in China has not yet been investigated systematically. In this study, profiles of 6,179 boreholes were collected from four regions in China, i.e., the Capital Metropolitan (CM), Xinjiang (XJ), Guangdong—Guangxi (GG), and Sichuan–Yunnan (SY) areas. Quantitative characteristic parameters including site category, equivalent shear wave velocity (V_{se}), and the thickness of the overlying soil layer (H) defined by the Chinese seismic code, and V_{S30} and the median shear wave profile were all analyzed to confirm the dependency on site conditions among the four regions. Investigation revealed that the majority of sites in most regions are classified as Class-II sites with no Class-IV sites, except in CM. In comparison with the other three regions, a larger number of GG sites are classified as Class-I. Sites in XJ are generally characterized by small H values (<20 m) and large V_{se} values (250 −450 m/s), while those in CM are characterized by large H values (average: ~50 m) and small V_{se} values (150 −300 m/s). Generally, the V_{se} and H values are similar in GG and SY, i.e., the sites are covered by an overlying soil layer that is ~20 m thick with an average V_{se} value of ~250 m/s. A very thin (<5 m) overlying soil layer is observed at many more sites in GG than at sites in the other three regions. The V_{S30} values in CM, SY, and GG all approximately follow a lognormal distribution with various logarithmic means, i.e., 257.2, 299.6, and 360.9 m/s, respectively. However, the V_{S30} values of most sites in XJ broadly follow a uniform distribution with a range of 200 −550 m/s. We summarized the characteristics of the median V_S profiles of each V_{S30}-based category (C1, C2, and C3) for each region. The median V_S profiles between any two regions are mainly manifested as parallel trends for sites in category C1, whereas they present trends of intersection for sites in categories C2 and C3. The findings of this study could serve as a basis for the establishment of a regional empirical model for site-dependent seismic response in China.

KEYWORDS

site condition, site borehole profiles, regional dependency, site category, V_{S30}

1 Introduction

The spatial distribution of ground motion is highly influenced by local site conditions, which can be determined on the basis of borehole profile characteristics that include the thickness of the overlying soil, shear wave velocity (V_S), and the geotechnical category and properties of each soil layer. Site effects are vital factors that must be considered in seismic design (e.g., GB 50011, 2010), seismic zonation (e.g., Mucciarelli, 2011), and ground motion predictions (e.g., Wen et al., 2018). Previous studies found that seismic response can vary markedly among sites with similar values of the time-weighted average shear wave velocity of the upper 30 m (V_{S30}) owing to substantial differences between borehole profiles (e.g., Ren et al., 2013; Rong et al., 2017). Qi et al. (2013) investigated the seismic response at sites with similar equivalent shear wave velocity and thickness of the overlying soil layer, and found notable dependency on the vertical arrangement of various soil layers. Kamai et al. (2016) observed obvious regional dependency of median V_S profiles in the same V_{S30} bin in three disparate regions (i.e., California, Taiwan, and Japan), and suggested the development of individual site-response prediction models for California and Japan.

Most previous related studies focused on verification of the regional dependency of soil dynamic parameters through dynamic testing of soil, which can provide important information for calculating site seismic response using the one-dimensional equivalent linear method (e.g., Yuan et al., 2000; Lv et al., 2003; Chen et al., 2005). On this basis, soil dynamic parameters have been recommended for use in various regions. However, few studies have addressed the regional dependency of site conditions. In regions with the same sedimentary environment and geological background, borehole profiles of the near-surface material should be broadly similar (Zhang et al., 2022). Theoretically, the borehole profiles vary from one region to another. Boore et al. (2011) found that the V_{S30} empirical estimation model developed for California (USA) is inapplicable to Japan because of substantial differences in borehole profiles. Wang et al. (2022) confirmed that commonly used V_{S30} extrapolation models are inapplicable to Xinjiang (China) owing to the special borehole profiles. Overall, no systematic studies have been performed previously to investigate the regional dependency of site conditions in China.

This study collected site borehole profiles in four regions of China, i.e., the Capital Metropolitan (CM), Xinjiang (XJ), Guangdong–Guangxi (GG), and Sichuan–Yunnan (SY) areas. We compared the site classes in each of the four regions, as defined on the basis of the Code for Seismic Design of Buildings of China (GB50011-2010) and three characteristic site parameters, i.e., the equivalent shear wave velocity (V_{se}), thickness of the overlying soil layer (H), and V_{S30}. We also compared the median V_S profiles for Class-II sites and sites categorized with the same V_{S30}–based category to investigate the potential dependency on site conditions among the four regions.

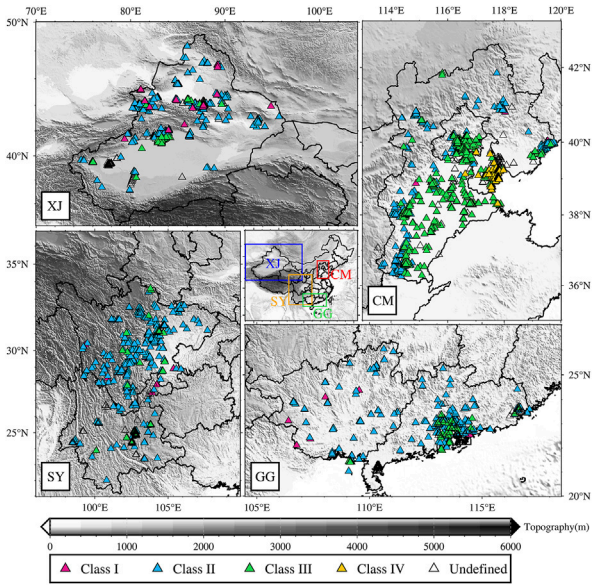

FIGURE 1
Locations of borehole sites in the four regions considered in this study, i.e., the Capital Metropolitan (CM), Xinjiang (XJ), Guangdong–Guangxi (GG), and Sichuan–Yunnan (SY) areas. Different colors are used to represent the various site classes defined by China's seismic code.

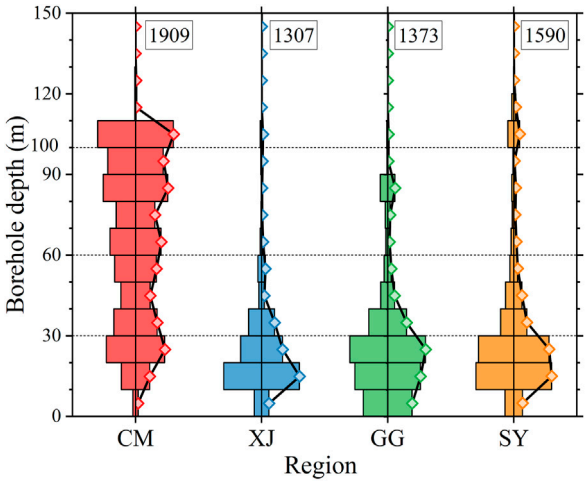

FIGURE 2
Histograms of the distribution of borehole depth at sites in CM, XJ, GG, and SY. The numbers within the box represent the total number of the sites in different regions, the rectangles with different colors stand for the number of sites in each bin, and the polylines with squares represent the proportion of the number of sites in each bin to the total.

The findings of this study could serve as the basis for establishment of a regional empirical model for site seismic response in China.

TABLE 1 Site categories defined by the Code for Seismic Design of Buildings of China (GB 50011, 2010).

Equivalent shear-wave velocity V_{se} (m·s^{-1})	Thickness of overlying soil layer, H (m)				
	I_0	I_1	II	III	IV
>800	0				
500 < V_{se} ≤ 800		0			
250 < V_{se} ≤ 500		<5	≥5		
150 < V_{se} ≤ 250		<3	3 ≤ H ≤ 50	>50	
≤150		<3	3 ≤ H ≤ 15	15 < H ≤ 80	>80

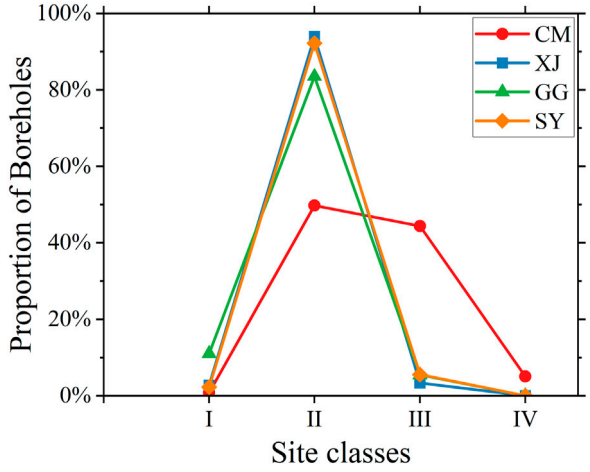

FIGURE 3
Proportions of borehole sites associated with different site classes in SY, XJ, GG, and CM.

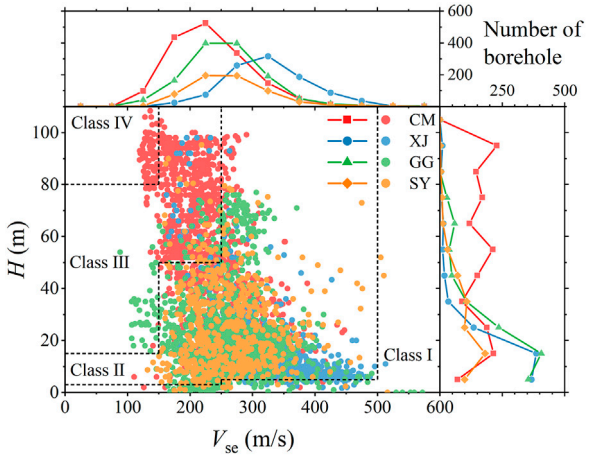

FIGURE 4
Scatter plots of V_{se} *versus* H for sites in CM, XJ, GG, and SY, together with histograms of V_{se} and H values. The polygonal lines distinguish the ranges of V_{se} and H for different site classes as defined by the Chinese seismic code.

2 Datasets

In total, 6,179 borehole profiles from sites in CM, XJ, GG, and SY were collected. The borehole profiles were mainly derived from the engineering site exploration, seismic safety evaluation, *etc.* The boreholes in CM, SY show a uniform spatial distribution. However, most boreholes in GG cluster in the Pearl River Delta Region, and boreholes in XJ are mainly spread along the north and south foot of Tianshan Mountain.

These profiles were then reorganized uniformly in terms of their geographic coordinates, V_S values, thickness, and the geotechnical category and properties of each soil layer. Figure 1 shows the geographical distribution of the borehole sites in China.

Figure 2 shows distribution histograms of the borehole depths at the sites in the four regions. The borehole depths at most sites are <30 m in XJ, GG, and SY, but a very small number of sites have borehole depths of >100 m. The sites in CM located on the North China Plain with a thick sedimentary layer have much deeper borehole depths, i.e., more than half the sites have borehole depths of >60 m, while a certain quantity have depths of >100 m.

In the Code for Seismic Design of Buildings of China (GB 50011, 2010), engineering sites are classified into four categories (Class-I, II, III, and IV) according to V_{se} and H, as listed in Table 1. Class-I sites include two subcategories (I_0 and I_1). In the code, V_{se} is defined as the time-weighted average V_S over the upper soil layer with minimum depth of 20 m and H. The code also definitely stipulates how to determine values of H according to various cases. Generally, H is defined as the depth to the upper surface of a soil layer for which V_S is not <500 m/s, and where the V_S value of the underlying soil layer is always not <500 m/s.

The V_{se} and H values were calculated according to the site borehole profiles and used to categorize the site classes. Note that some boreholes were not included in the following analysis because the H values were unascertainable owing to the limited number of borehole depths. Figure 3 shows the proportion of sites divided into

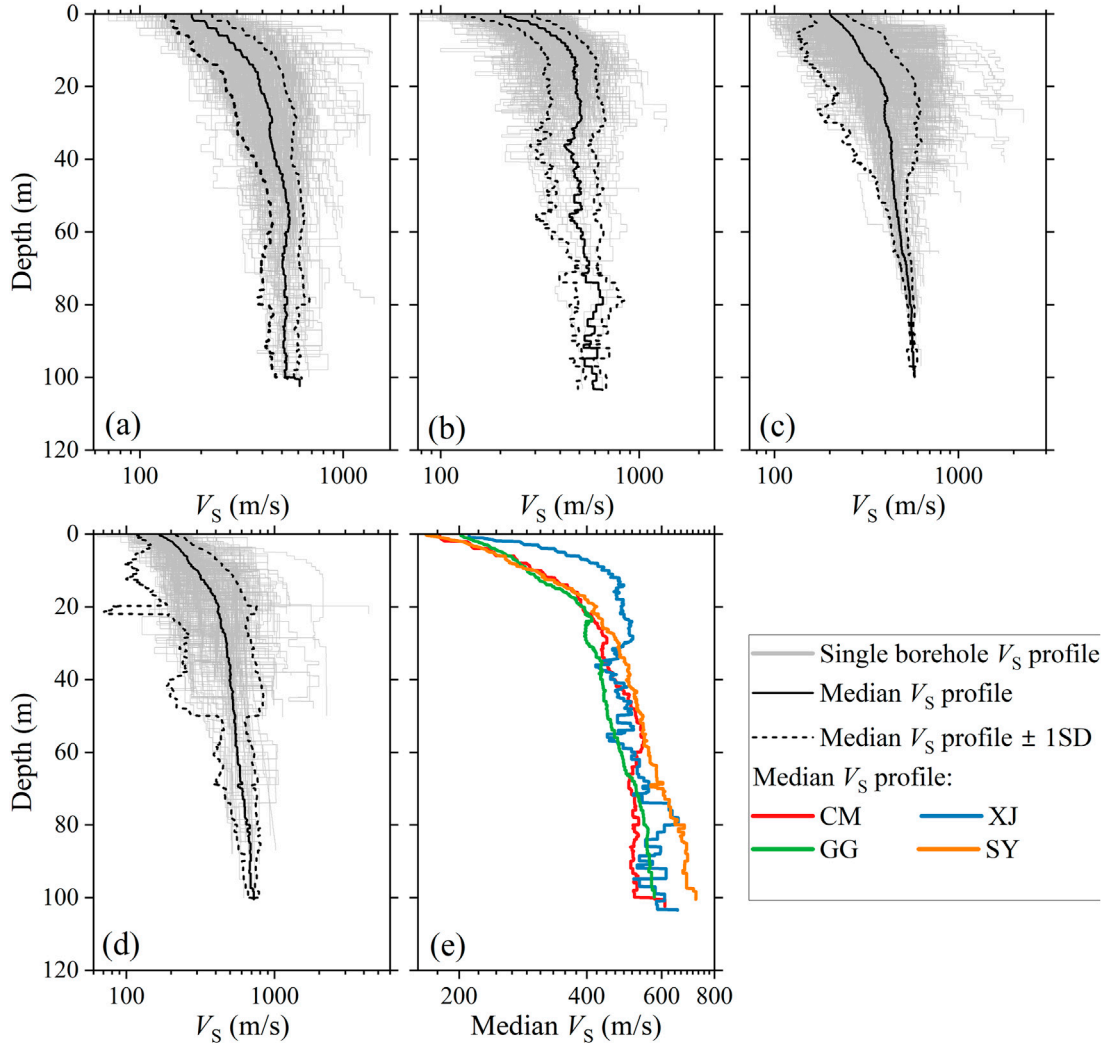

FIGURE 5
The V_S profiles of Class-II sites in **(A)** SY, **(B)** GG, **(C)** CM, and **(D)** XJ areas. Solid and dotted lines indicate the median V_S profile and the one standard deviation range, respectively, for each region. **(E)** The median V_S profiles of the Class-II sites in the four regions are compared in panel.

the various site classes for the four regions. The overwhelming majority of sites in XJ, GG, and SY are classified as Class-II sites, while only a few are classified as Class-I and Class-III sites. No site in XJ, GG, or SY is assigned to the Class-IV group. We also note that the proportion of Class-I sites in GG is substantially higher than that in either XJ or SY. In contrast, in CM, the number of Class-III sites is slightly lower than that of Class-II sites, and Class-II and Class-III sites account for the majority. In CM, some sites are classified as Class-IV sites, and their proportion is far greater than that of the Class-I sites. As shown in Figure 1, the Class-III and Class-IV sites in CM are generally distributed around the coastal area with very soft and deep soils. The common characteristic that Class-II sites account for the majority is also the result determined using the Chinese seismic code with a wide interval of Class-II sites.

3 Regional dependency of site conditions

3.1 Regional dependency of H and V_{se}

Figure 4 presents V_{se}–H scatter plots for the four studied regions, together with histograms of the H and V_{se} values. The H values of XJ sites are generally <20 m, while the V_{se} values are at a comparatively high level (250 –450 m/s), indicating that most sites in XJ are covered by thin and hard soil (e.g., sand and silty clay). In contrast, CM sites generally show an approximately uniform distribution of H values in the range of 0 –100 m (average: ~50 m) and lower V_{se} values in the range of 150 –300 m/s, indicating deep and soft surficial soil. The

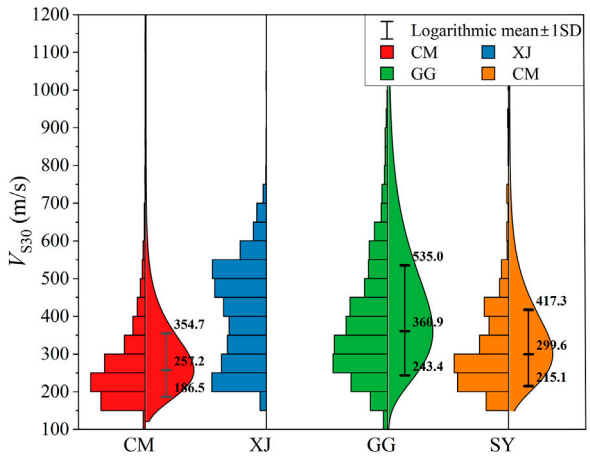

FIGURE 6
Frequency distributions of V_{S30} values in the four studied regions.

V_{se}–H scatter plots present similar distributions for GG and SY. Generally, the ground surface in both regions is covered by an overlying soil layer that is ~20 m thick with an average V_{se} value of ~250 m/s. However, in comparison with the other three regions, the overlying soil layer is very thin (<5 m) at many more sites in GG. In comparison with those sites with a very deep overlying soil layer (i.e., >80 m) in XJ, CM, and SY, some of the sites in CM are characterized by very low V_{se} (i.e., <150 m/s), and sites with higher V_{se} values account for a larger proportion of such sites in SY. The above results fully reflect the major differences in H and V_{se} at the various sites in the four studied regions.

3.2 Regional dependency of V_S profiles

The potential regional dependency in the V_S profiles was investigated based on the boreholes of the Class-II sites in the four regions. Figure 5 shows the variation of V_S with depth for each Class-II site, as well as the V_S median and the one standard deviation range for each region. Very obvious differences are evident in the V_S profiles of the Class-II sites in the four regions. The median V_S profiles for the four regions are also plotted in Figure 5 for comparison purposes. The sites in the four regions show some similarities in terms of the characteristics of the variation in median V_S with depth, i.e., a sharp increase in V_S in shallow soil layers from the ground surface to a critical depth, and notably slower increase in deeper soil layers beneath the critical depth. The differences in the median V_S profiles for the four regions were investigated. The median V_S profile in XJ shows a much shallower critical depth (~13 km) than that in the other three regions (~20 km). The median V_S values (increasing from ~220; to ~480 m/s) in the shallow soil layers in XJ are much larger than those (increasing from ~200; to ~400 m/s) in the other regions. The median V_S value in XJ appears to exhibit faster increase in shallow soil depths than that in the other regions. The median V_S values of the deeper soil layers in XJ generally show no

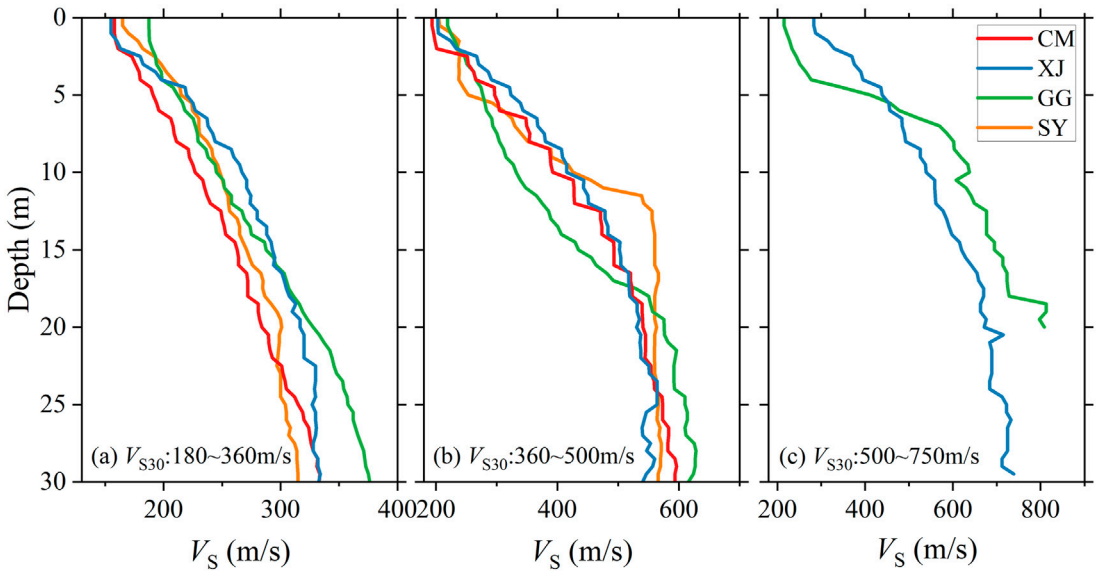

FIGURE 7
Median V_S profiles for sites belonging to each V_{S30}-based category in the four regions considered in this study: **(A)** category C1 for V_{S30} = 180–360 m/s, **(B)** category C2 for V_{S30} = 360–500 m/s, and **(C)** category C3 for V_{S30} = 500–750 m/s.

TABLE 2 Trends describing the regional dependency between any two regions for each V_{S30}-based site category.

	Sites within C1 category			Sites within C2 category			Sites within C3 category		
	XJ	GG	SY	XJ	GG	SY	XJ	GG	SY
CM	○	○	×	●	×	×			
XJ		×	○		×	×		×	
GG			○			×			

Noting ○ indicates the parallel median V_S profiles, ● indicates the overlapped median V_S profiles, and × indicates the intersecting median V_S profiles.

obvious increase with depth. Such a phenomenon is also observed in many of the deeper soil layers (>60 m) in CM. In GG and SY, the median V_S values of the deeper soil layers maintain continuous increase with depth, i.e., from 400; to 580 m/s and to 700 m/s, respectively. Our results indicate that it is necessary to consider regionally dependent site amplification effects in seismic design.

3.3 Regional dependency of V_{S30}

Although the Chinese seismic code uses site categories to characterize the effects of local site conditions on ground motions, V_{S30} is also an important parameter commonly used to characterize local site amplification. The potential regional dependency of V_{S30} was further investigated on the basis of the borehole data from the four studied regions. The V_{S30} values were estimated for sites with borehole depths of <30 m using the constant extrapolation model (Wang et al., 2022) if a rock layer was situated at the bottom of the borehole, and using the linear extrapolation model if a soil layer was situated at the bottom of the borehole.

Frequency distributions of the V_{S30} values in the four studied regions are plotted in Figure 6. The V_{S30} distributions in CM, SY, and GG all approximately follow a lognormal distribution with logarithmic means of 257.2, 299.6, and 360.9 m/s, respectively. The range of one standard deviation in CM, SY, and GG is 186.5–354.7, 215.1–417.3, and 243.4–535.0 m/s, respectively, indicating that the near-surface soil layer in the upper 30 m is on average hardest in GG and softest in CM. The V_{S30} values at a certain proportion of sites in GG are measured or estimated to be >800 m/s, corresponding to hard soil or rock sites, while barely any such sites are found in CM. However, the near-surface site conditions in CM could be confirmed to be most similar owing to the narrowest dispersion of V_{S30} values, while the widest dispersion in GG indicates greatest discrepancy. Different from the other three regions, the V_{S30} values of XJ sites do not follow a lognormal distribution. Instead, the V_{S30} values for most sites fall within a wide range of 200 –550 m/s, approximately following a uniform distribution with an average of ~400 m/s.

The V_{S30}-related empirical relations are often used to characterize site amplification effects, e.g., in predicting ground motions. Moreover, the empirical relations associated with site categories are also used (e.g., Bindi et al., 2011). However, in such cases, the same amplification effects appear associated with sites belonging to the same site category but with different measured V_{S30} values. Therefore, we explored the potential regional dependency of V_{S30} values measured or estimated at sites belonging to the same site category. Referring to the seismic code of China and other countries and regions, most sites considered in this study were divided into three categories on the basis of the V_{S30} values, i.e., C1 for V_{S30} = 180 –360 m/s, C2 for V_{S30} = 360 –500 m/s, and C3 for V_{S30} = 500 –750 m/s.

The median V_S profiles for sites belonging to each category were computed for each of the four regions and illustrated in Figure 7. Note that the median V_S profiles for sites within category C3 in SY and CM are not presented owing to the limited number of samples which is less than 10% of the total number of sites. Substantial regional dependency is also observed in the median V_S profiles of sites within the same category. To clearly express the regional dependency of median V_S profiles of each category, we defined three trends to describe the regional dependency between any two regions considered in this study, i.e., 1) parallel median V_S profiles between two regions that indicate similar V_S variation with depth and greater V_S values in one region in comparison with those in another; 2) intersecting median V_S profiles of two regions that indicate dissimilar V_S variation with depth and greater (lower) V_S in the upper (lower) soil layers in one region in comparison with those in another; and 3) overlapping median V_S profiles at certain depths for both regions indicating consistent V_S values. The three trends between any two regions for each V_{S30}-based site category are listed in Table 2. For sites belonging to category C1, the median V_S profiles between two regions are mainly manifested as a parallel trend, while a trend of intersection appears for XJ–GG and XJ–SY pairings. However, for sites belonging to categories C2 and C3, the median V_S profiles between two regions are predominantly shown as intersection trends, while only the XJ–CM pairing in category C2 shows as an overlapping trend. It is worth noting that the median V_S profiles for categories C2 show an intersection trend with the other three regions and categories C3 intersect with XJ in GG. The median V_S values of the upper soil layers in GG are relatively

small but relatively large in the lower soil layers, reflecting the higher impedance ratio and the corresponding stronger site seismic responses in GG. The trends of the median V_S profiles for the same V_{S30}-based category between any two regions fully demonstrate the regional dependency of the V_{S30} values measured or estimated at sites belonging to the same site category. Even if the V_{S30} values among the four regions are similar, the V_S profiles can differ substantially, which could cause huge differences in site seismic responses.

4 Conclusion

This study collected over 6,000 borehole profiles from sites in four regions (i.e., XJ, CM, GG, and SY) in China to investigate the potential regional dependency of site conditions. These sites were first classified into corresponding site categories as defined by the Chinese seismic code. The regional dependencies in V_{se}, H, and V_{S30}, and also in the V_S profiles, were clearly observed at the various sites among the four regions. The following conclusions were drawn.

1) The proportion of Class-II sites is the highest among all four regions. Sites in XJ are generally characterized by small H values (<20 m) and large V_{se} values (250 –500 m/s); conversely, the H values are large and the V_{se} values are small in CM. Except for XJ sites, the V_{se} values all follow a Gaussian distribution with an average of ~250 m/s. The H values in CM exhibit an approximately uniform distribution in the range of 0 –100 m, while those in other regions are concentrated mainly in a range of 0 –30 m.
2) The V_{S30} values for the majority of sites in CM and SY are not >500 m/s, while some sites in XJ and GG show high V_{S30} values in the range of 500 –750 m/s. Except for XJ sites, the V_{S30} values in CM, SY, and GG all approximately follow a lognormal distribution with a logarithmic means of 257.2, 299.6, and 360.9 m/s, respectively. However, the V_{S30} values of XJ sites fall mainly within a wide range of 200 –550 m/s.
3) We defined three trends to describe the regional dependency of the median V_S profiles of each V_{S30}-based category (i.e., C1, C2, and C3) between any two regions. For sites belonging to category C1, C2 and C3, the median V_S profiles between two regions are manifested as a trend of parallel and intersection, respectively. The median V_S values of the upper soil layers in GG are relatively small but relatively large in lower soil layers, reflecting the higher impedance ratio and the corresponding stronger site seismic responses in GG.

The above conclusions were obtained statistically using available borehole data that represent the average characteristics of site conditions in the studied regions. These results might be subject to change when additional borehole data are incorporated in the future. However, the regional dependency of site conditions is evident, and it is recommended that it should be considered in seismic zonation mapping and seismic design codes.

Data availability statement

The original contributions presented in the study are included in the article/supplementary material, further inquiries can be directed to the corresponding author.

Author contributions

XY analyzed the data, interpreted the results, and drafted the manuscript. PZ encoded the borehole data, interpreted the results, and corrected the manuscript. YZ processed the borehole data and corrected the manuscript. HW collected the borehole data and reviewed the manuscript. DW processed the borehole data. All authors read and approved the final manuscript.

Funding

This work is supported by National Key R&D Program of China under grant number 2019YFE0115700; Chinese National Natural Science Fund under grant number 51878632; Natural Science Foundation of Heilongjiang Province under grant number YQ2019E036; Heilongjiang Touyan Innovation Team Program.

Conflict of interest

The authors declare that the research was conducted in the absence of any commercial or financial relationships that could be construed as a potential conflict of interest.

Publisher's note

References

Bindi, D., Pacor, F., Luzi, L., Puglia, R., Massa, M., Ameri, G., et al. (2011). Ground motion prediction equations derived from the Italian strong motion database. *Bull. Earthq. Eng.* 9, 1899–1920. doi:10.1007/s10518-011-9313-z

Boore, D. M., Thompson, E. M., and Cadet, H. (2011). Regional correlations of V_{S30} and velocities averaged over depths less than and greater than 30 meters. *Bull. Seismol. Soc. Am.* 101 (6), 3046–3059. doi:10.1785/0120110071

Chen, G. X., Liu, X. Z., Zhu, D. H., and Hu, Q. X. (2005). Study on dynamic characteristics of recently deposited soils in southern area of jiangsu Province. *Chin. J. Undergr. Space. Eng.* 1 (7), 1139–1142. (in Chinese with English abstract). doi:10.3969/j.issn.1673-0836.2005.z1.042

GB 50011 (2010). *Code for seismic design of buildings*. Beijing: China Architecture Industry Press. (in Chinese).

Kamai, R., Abrahamson, N. A., and Silva, W. J. (2016). V_{S30} in the NGA GMPEs: Regional differences and suggested practice. *Earthq. Spectra.* 32 (4), 2083–2108. doi:10.1193/072615EQS121M

Lv, Y. J., Tang, R. Y., and Sha, H. J. (2003). Experimental study on dynamic shear modulus ratio and damping ratio of the soils of bohai seafloor. *J. Disaster. Prev. Mitig. Eng.* 23 (2), 368–374. (in Chinese with English abstract). doi:10.13409/j/cnki.jdpme.2003.02.006

Mucciarelli, M. (2011). Ambient noise measurements following the 2011 christchurch earthquake: Relationships with previous microzonation studies, liquefaction, and nonlinearity. *Seismol. Res. Lett.* 82 (6), 919–926. doi:10.1785/gssrl.82.6.919

Qi, W. H., Liu, H. S., and Bo, J. S. (2013). A new site classification index: Equivalent period of soil layer. *Earthq. Eng. Eng. Dyn.* 33 (6), 228–235. (in Chinese with English abstract). doi:10.13197/j.eeev.2013.06.228.qiwh.032

Ren, Y. F., Wen, R. Z., Yamanaka, H., and Kashima, T. (2013). Site effects by generalized inversion technique using strong motion recordings of the 2008 Wenchuan earthquake. *Earthq. Eng. Eng. Vib.* 12 (02), 165–184. doi:10.1007/s11803-013-0160-6

Rong, M. S., Fu, L. Y., Wang, Z., Li, X. J., Carpenter, N. S., Woolery, E. W., et al. (2017). On the amplitude discrepancy of HVSR and site amplification from strong-motion observations. *Bull. Seismol. Soc. Am.* 107 (6), 2873–2884. doi:10.1785/0120170118

Wang, D. R., Ren, Y. F., Zhang, Y. T., Ji, K., Wang, H. W., and Wen, R. Z. (2022). Method for correcting extrapolation model of engineering site parameter V_{S30}. *J. Harbin. Inst. Technol. Online Publ.* (in Chinese with English abstract). doi:10.11918/202110086

Wen, R. Z., Xu, P. B., Wang, H. W., and Ren, Y. F. (2018). Single-station standard deviation using strong-motion data from sichuan region, China. *Bull. Seismol. Soc. Am.* 108 (4), 2237–2247. doi:10.1785/0120170276

Yuan, X. M., Sun, R., Sun, J., Meng, S. J., and Shi, Z. J. (2000). Laboratory experimental study on dynamic shear modulus ratio and damping ratio of soils. *Earthq. Eng. Eng. Dyn.* 20 (4), 133–139. (in Chinese with English abstract). doi:10.13197/j.eeev.2000.04.020

Zhang, Y. T., Ren, Y. F., Wen, Z., and Wang, D. R. (2022). A method of site parameter estimation based on decision tree theory considering terrain features. *Chinses J. Geophys.* 65 (2), 698–710. (in Chinses with English abstract). doi:10.6038/cjg2022P0021